Electric and Magnetic Field Minimization using Optimal Phase Arrangement Techniques for MEA Overhead Power Transmission Lines

Suthasinee Nunchuen† and **Vuttipon Tarateeraseth**, Non-members

ABSTRACT

In order to minimize the electric and magnetic fields generated by Metropolitan Electricity Authority (MEA) overhead power transmission lines, optimal phase arrangement techniques were applied for 3-circuit overhead power transmission lines (69/230 kV). In this paper, a mathematical model was designed using a MATLAB program. Its correctness was validated by comparing the simulated results with measured results from the South Thonburi power transmission lines at Rama 2 Road (outbound side). Both were evaluated with the same conditions. We show that optimal phase arrangement techniques can minimize the generated electric and magnetic fields, lowering them so they are less than the safe limits given by the World Health Organization.

Keywords: Phase Arrangements, Electric Field, Magnetic Field, Overhead Power Transmission Lines

1. INTRODUCTION

Nowdays, the Metropolitan Electricity Authority (MEA) in Thailand has been installing power transmission lines taking into account the generated electric and magnetic fields to address safety concerns according to the World Health Organization (WHO) [1]. Various research efforts have been focusing on the possibility of health effects from extremely low frequency (ELF) electromagnetic fields (EMF). The WHO and International Commission on Non-Ionizing Radiation Protection (ICNIRP) have released human safety limits for ELF-EMF as shown in Table 1 [1, 2]. It is worth noting that the electric field from the natural areas near the earth is normally less than 200 V/m and may be as high as 50 kV/m during lightning strikes. Theoreticality speaking, when one stands under a high-voltage overhead transmission line, the electric field can pass through the whole body. The electric charge distributes over the surface of the whole body causing electricity to flow through the body to the ground [3]. Magnetic field radiates around power transmission lines; their impact on human brain is negative [4]. Furthermore, the electric and magnetic fields are also used in medicine to diagnose and treat various diseases [5, 6]. A human body is more sensitive to magnetic field than to electric field [2, 7]. For those who have been exposed to intense and prolonged ELF-EMF, they should be aware that it can increase the risk of leukemia, cancers, and neurodegenerative diseases, etc. This is especially true for children [8–10]. However, currently, there is no clear evidence to be allow reaching a definitive conclusion [11–13]. Therefore, much research has been proposing various approaches in order to reduce the electric field values generated by overhead power transmission lines that are encountered in everyday life.

R. M. Sarmento [14] presented a charge simulation method to calculate the electric and magnetic fields generated by 400 kV overhead power lines at Batalha-Pego [15]. The simulated results were validated by comparing with the measured results. It showed the good agreement between them.

S. S. Razavipour *et al.* [16] used two different methods to evaluate the electrical field quantities. The Semi-numerical method uses the laws of electrostatic techniques to simulate the two-dimensional electric field under the high-voltage overhead transmission lines, and the finite element method (FEM) uses specific boundary conditions to compute the two-dimensional electric field. FEM provided more accurate results. In [17], the electric field distribution of a high-voltage overhead transmission line has been analyzed with 2 different approaches, one using 2-D FEM or boundary element method (BEM), and another with an analytical method using the formulas derived from full expression of Maxwell's equations [18]. The simulated results were compared with the measured values obtained on double-circuit 400-kV transmission lines. The experiment showed a good agreement of the results.

A. Diamantis and A. G. Kladas [19] developed a mix of 3-D FEM, analytical solutions, and equivalent surface impedance methodology for the computation

Manuscript received on September 23, 2019 ; revised on August 5, 2020 ; accepted on August 7, 2020. This paper was recommended by Associate Editor Kriangkrai Sooksood.

The authors are with the Faculty of Engineering, Department of Electrical Engineering, Srinakharinwirot University, Ongkharak, Nakhon Nayok, Thailand.

†Corresponding author: suthasinee.nunchuen@g.swu.ac.th

Digital Object Identifier 10.37936/ecti-eec.2021191.217575

Table 1: *Maximum exposure limits of electromagnetic fields at 50 Hz [1, 2].*

Category	Electric field (kV/m)	Magnetic field (mG)
Public	5	1,000
Occupational	10	5,000

of electric and magnetic fields distributions under single-circuit 400 kV overhead transmission lines. The conductors are carrying rms phase currents of 1000 A at height of 1.5 m from the ground. The analytical formulas of electric and magnetic fields were applied by Coulomb's and Biot– Savart's laws, respectively [20]. The computed values were practically half of the admissible limits of ICNIRP [2]. In [21], the authors proposed to find the optimal phase arrangement techniques only for the electric field generated by MEA overhead power transmission lines where the generated magnetic field was ignored. As a result, the main contribution of this paper is to expand the works of [21] by proposing optimal phase arrangement techniques that provide the minimum of both electric and magnetic fields for MEA overhead power transmission lines using an analytical approach. Moreover, to verify the accuracy of our proposed technique, the simulated results were compared with the experimental results.

2. MATHEMATICAL FORMULATIONS OF ELECTRIC FIELD AND MAGNETIC FIELD BY OVERHEAD POWER TRANSMISSION LINES

2.1 Electric field

To reduce the calculation complexity, the electric field generated by overhead power transmission lines were computed using analytical approach. The simulation considered the 69 kV and 230 kV overhead power transmission lines as infinite line charges. Fig. 1 shows the layout of overhead transmission lines to calculate the electric field. To represent the three-phase transmission line systems, there are three infinite line charges A, B, and C placed at positions (x_1, y_1), (x_2, y_2), and (x_3, y_3), respectively. Each of the conductors is a straight line and they parallel to each other and to the ground plane. According to the image theory, there are three infinite line charges A', B', and C' placed at positions (x_1, y_1), (x_2, y_2), and (x_3, y_3) under the ground plane. However, to simplify the calculation, the following assumptions were made [22].

- The refraction of the electric field was ignored.
- The sag lines between the pole and the deduction of the conductors are also neglected.

With the mentioned assumptions, the electric field ($\vec{E}$) at point $P(x_c, y_c)$ can be derived as shown in Eq. (1) [23].

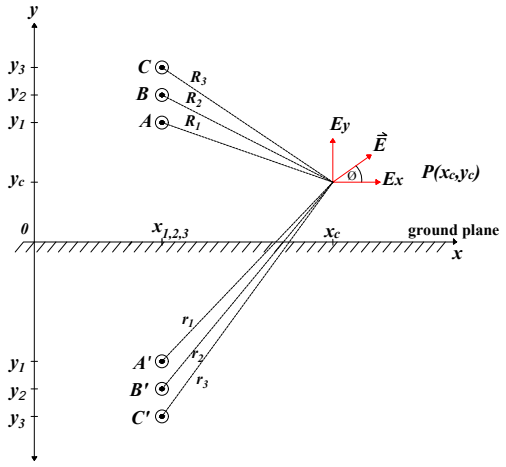

Fig.1: *Layout of overhead transmission lines for electric field calculations.*

$$\vec{E} = \frac{V}{R \ln(\frac{y}{a})}(\sin\theta\vec{a}_x + \cos\theta\vec{a}_y) \tag{1}$$

where $\vec{E}$ is the generated electric field (kV/m). V is phase voltage (V). y is the distance between the earth and line conductors (m). a is radius of the line conductors (m). $\vec{a}_x$ and $\vec{a}_y$ are the unit vector along the x-axis and y-axis, respectively.

Assuming that the ground is perfectly infinite conducting plane, the electric field at point $P(x_c, y_c)$ generated by six infinite line charges A, B, C, A', B', and C' can be decomposed into 6 parts as follows:

$$\vec{E}_A = \frac{V_1}{R_1 \ln(\frac{y_1}{a})}(\sin\theta\vec{a}_x + \cos\theta\vec{a}_y) \tag{2}$$

$$\vec{E}_B = \frac{V_2}{R_2 \ln(\frac{y_2}{a})}(\sin\theta\vec{a}_x + \cos\theta\vec{a}_y) \tag{3}$$

$$\vec{E}_C = \frac{V_3}{R_3 \ln(\frac{y_3}{a})}(\sin\theta\vec{a}_x + \cos\theta\vec{a}_y) \tag{4}$$

$$\vec{E}_{A'} = \frac{-V_1}{r_1 \ln(\frac{y_1}{a})}(\sin\theta\vec{a}_x + \cos\theta\vec{a}_y) \tag{5}$$

$$\vec{E}_{B'} = \frac{-V_2}{r_2 \ln(\frac{y_2}{a})}(\sin\theta\vec{a}_x + \cos\theta\vec{a}_y) \tag{6}$$

$$\vec{E}_{C'} = \frac{-V_3}{r_3 \ln(\frac{y_3}{a})}(\sin\theta\vec{a}_x + \cos\theta\vec{a}_y) \tag{7}$$

where V_1, V_2, and V_3 are phase voltage (V). x_c and y_c are the distance from the point (0,0) to point of considering the electric field at point $P(x_c, y_c)$ (m). R is the distance from each cables to the point $P(x_c, y_c)$ (m). r is the distance between the image conductor and the observation point $P(x_c, y_c)$ (m).

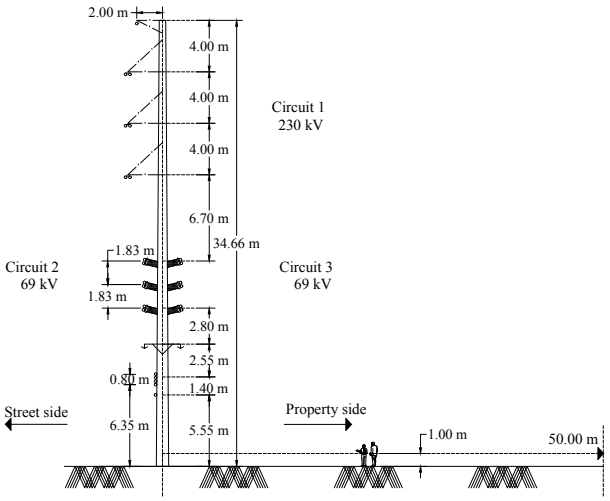

Fig.2: *Layout of measuring point of overhead transmission lines.*

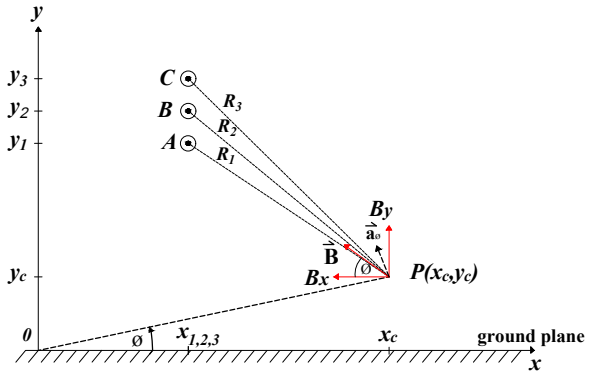

Fig.3: *Layout of overhead transmission lines for magnetic field calculations.*

From Eqs. (2)–(7), the total electric field generated by the overhead power transmission lines A, B, and C, including the image projection of A', B', and C' from Fig. 1, can be found with Eq. (8).

$$E_{total} = \left|\vec{E}_A + \vec{E}_{A'} + \vec{E}_B + \vec{E}_{B'} + \vec{E}_C + \vec{E}_{C'}\right| \quad (8)$$

2.2 Magnetic field

Similarly, in order to formulate the generic equation of the magnetic fields caused by MEA overhead power transmission lines, the physical model was converted into a mathematical model as shown in Fig. 3. To simplify the calculation complexity of the magnetic flux density ($\vec{B}$) at point $P(x_c, y_c)$, the following assumptions were made.

- The earth has no effect on the magnetic field produced by the overhead power transmission lines.
- The total magnetic field at any point is determined by linear superposition of the magnetic field produced by the currents flowing in each individual conductor and can be combined into a vector.
- The effect of induced shield/sheath currents on the magnetic field is negligible.
- The lines were considered to be infinitely long and linear.
- The current through the conductors flows out of the paper.

The magnetic flux density $\vec{B}$ is related to the circuit current I as shown in Eq. (9).

$$\vec{B} = \frac{\mu_0 \mu_r I_c}{2\pi R}\vec{a}_\phi \quad (9)$$

where $\vec{B}$ is the magnetic flux density produced by each conductor (T). I_c is current flowing through an individual conductor where its direction is out of the paper (A). R is the distance from each line to the point $P(x_c, y_c)$ (m). μ_r is the relative permeability. μ_0 is the permeability of free space (H/m).

As shown in Fig. 3, the magnetic field density can be decomposed into two parts along the x-axis and y-axis as shown in Eqs. (10) and (11).

$$B_x = -\frac{\mu_0\mu_r}{2\pi}\left[\frac{(y_1 - y_c)I\angle 0^\circ}{(x_c - x_1)^2 + (y_1 - y_c)^2} + \frac{(y_2 - y_c)I\angle 120^\circ}{(x_c - x_2)^2 + (y_2 - y_c)^2} + \frac{(y_3 - y_c)I\angle 240^\circ}{(x_c - x_3)^2 + (y_3 - y_c)^2}\right] \quad (10)$$

$$B_y = \frac{\mu_0\mu_r}{2\pi}\left[\frac{(x_c - x_1)I\angle 0^\circ}{(x_c - x_1)^2 + (y_1 - y_c)^2} + \frac{(x_c - x_2)I\angle 120^\circ}{(x_c - x_2)^2 + (y_2 - y_c)^2} + \frac{(x_c - x_3)I\angle 240^\circ}{(x_c - x_3)^2 + (y_3 - y_c)^2}\right] \quad (11)$$

From Eqs. (10) and (11), the total magnetic flux density produced by three-phase current flowing through the MEA overhead power transmission lines can be found with Eq. (12).

$$B = \sqrt{B_{xr}^2 + B_{xi}^2 + B_{yr}^2 + B_{yi}^2} \quad (12)$$

where B_{xr} and B_{xi} are the real and imaginary parts of B_x, whereas B_{yr} and B_{yi} are the real and imaginary parts of B_y, respectively.

3. EXPERIMENTAL VALIDATIONS

The generated electric and magnetic fields were measured at the South Thonburi power transmission lines, Rama 2 road (outbound side). Practically, the electric and magnetic fields were measured using a

Fig.4: *Installation of electricity recorder of overhead transmission lines [22].*

Fig.5: *Electric and magnetic fields measurement setup at South Thonburi [22].*

monopole antenna as a starting point. The monopole antenna was placed 1 m above ground [22, 24] as shown in Figs. 4–5. The measurement was recorded every 1 m with a total distance of 50 m with an ELF survey meter (Holaday, HI-3604) where the frequency response is in the range of 50 up to 1000 Hz. It can measure the electric field from 1 V/m to 199 kV/m, and the magnetic field from 0.1 mG to 20 G. It was deployed with a three-leg stand model 491009 Dielectric Tripod, recording the current of the MEA overhead power transmission lines using a supply network analyser AR5 and a LEM TOPAS 1000 [22, 25].

3.1 Electric field

The electric field has been evaluated using derived formulas as shown in Section 2.1. The simulated results by MATLAB were validated by comparing them with the measured results under the same conditions. The line-to-line voltages are 69 kV and 230 kV. The installation patterns are shown in Fig. 2.

The mathematical simulation was designed using derived equations, Eqs. (1)–(8), and implemented by a MATLAB Program. It should be noted that the calculation used the same assumptions as the measurements.

Figs. 6 and 7 show the comparison of the electric field of the MEA overhead power transmission lines before and after applying our phase arrangement technique. That measurement was considered to be at a height of 1 m above ground to allow comparison between simulated and measured results. The result graphs show a good agreement of the results. The value obtained from the simulation of the electric field is higher than the value from the measurement by

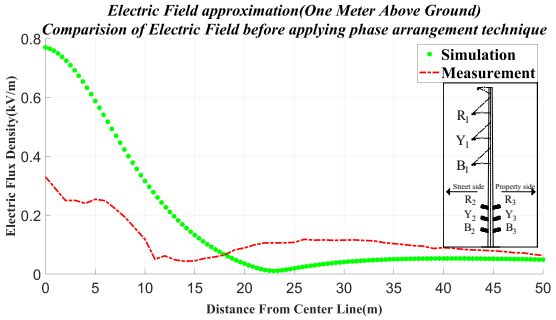

Fig.6: *Comparison of electric field produced by 3-circuit overhead power transmission lines before applying phase arrangement technique between the simulation and the actual measured values.*

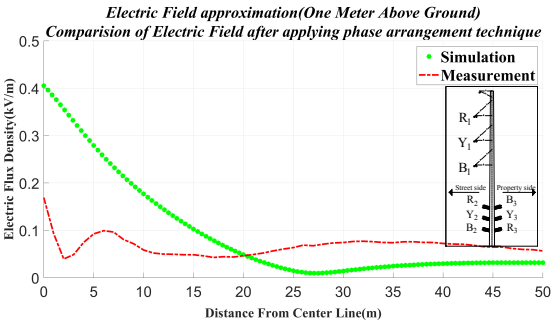

Fig.7: *Comparison of electric field produced by 3-circuit overhead power transmission lines after applying phase arrangement technique between the simulation and the actual measured values.*

about 0.4 kV/m at position (0,0). These error values depend on many factors such as real environment, metal fences, trees, towers, electric poles, etc. All mentioned factors can have an affect on the refraction of the electric field.

3.2 Magnetic field

To assure the accuracy of the derived equations of the magnetic fields produced by 3-circuit overhead power transmission lines (69/230 kV), the simulated results and the measuerd results were compared under the same conditions. The magnetic field was investigated with a 3-circuit installation as shown in Fig. 2. The magnetic field generated by the MEA overhead power transmission lines was measured at a height of 1 m above the ground. The distance at x-axis varied from 0 to 50 m and measurements were taken by an ELF survey meter (Holaday, HI-3604).

For the MATLAB simulation using Eqs. (9)–(12), the same conditions as existed at the measurement test site were chosen.

Figs. 8 and 9 show the comparison between simulated and measured results of the magnetic field generated by MEA overhead power transmission lines before and after applying phase arrangement techniques. They are comparing the magnetic field

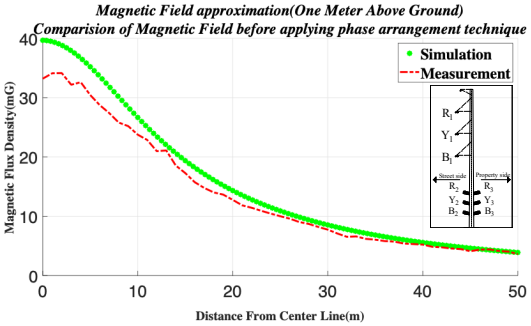

Fig.8: *Comparison of magnetic field produced by 3-circuit overhead power transmission lines before applying phase arrangement technique between the simulation and the actual measured values.*

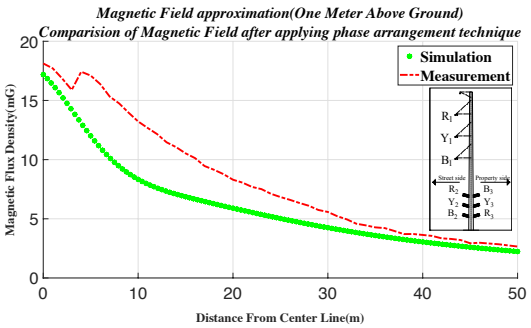

Fig.9: *Comparison of magnetic field produced by 3-circuit overhead power transmission lines after applying phase arrangement technique between the simulation and the actual measured values.*

at 1 m height above the ground level for 69 kV and 230 kV overhead power transmission lines. The resulting graphs have shown a positive outcome.

Since the magnetic field depends on the current of the transmission lines, Table 2 shows that the average current values which were measured before and after phase arrangement techniques have different values. Therefore, the maximum value of the measured currents was used to find the best and the worst cases of both electric and magnetic fields after phase arrangement techniques were applied.

Table 2: *Measured current of the MEA overhead power transmission lines*

The measured current values by MEA (A)		
Circuits	Before applying phase arrangement technique	After applying phase arrangement technique
1	550	590
2	440	500
3	370	515

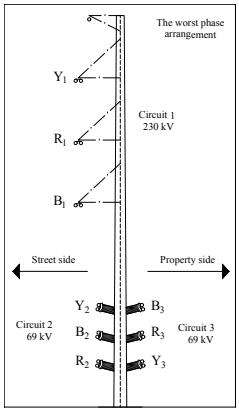

Fig.10: *Maximum electric field value provided by the worst phase arrangement.*

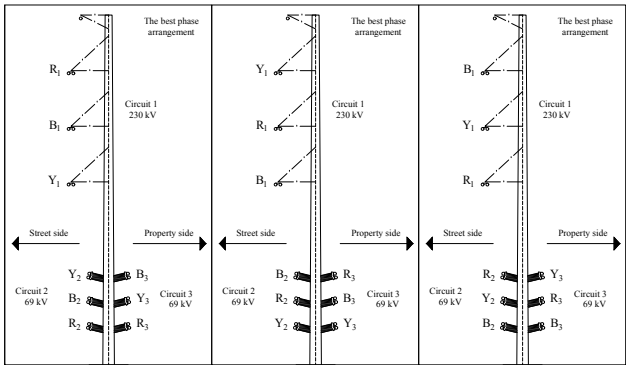

Fig.11: *Proposed best phase arrangements which provide the minimum electric field.*

4. APPROPRIATE PHASE ARRANGEMENT PATTERNS

Normally, there are three types of installations: 1-circuit, 2-circuit, and 3-circuit. In this paper, only 3-circuit cases were investigated. The line-to-line voltage of circuit#1 was 230 kV, whereas circuit#2 and circuit#3 were 69 kV as shown in Fig. 2.

4.1 Electric field

When using Eqs. (1)–(8) to find the optimal phase arrangement techniques of the electric field produced by MEA overhead power transmission lines, before investigation what patterns provide the minimum electric field, the following assumptions must be defined.

- We consider the electric field to be at 1 m above ground level, where the x-coordinate range varies from 0 to 50.
- We ignore both ground and neutral currents.

All possible phase arrangements of 3-circuit that provide the maximum and minimum electric field values are summarized as shown in Figs. 10 and 11, respectively. In addition, Fig. 12 shows the comparisons of electric field produced by 3-circuit overhead power transmission lines after applying phase arrangement techniques between the best and worst phase arrangements. The worst phase

Table 3: *The optimal phase arrangement techniques*

Phase arrangements	Electric field (kV/m)	Magnetic field (mG)
The worst	2,241	48.83
The best	0.03738	10.72

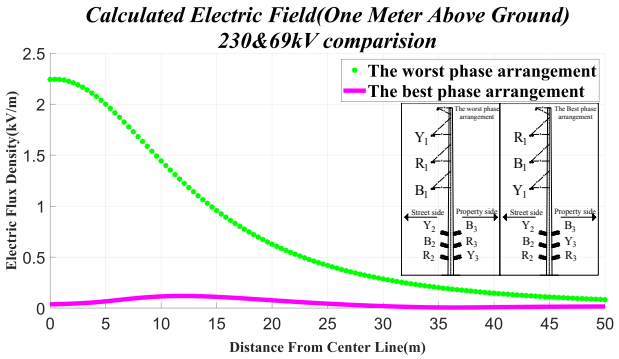

Fig.12: *Comparison of electric field produced by 3-circuit overhead power transmission lines after applying phase arrangement technique between the best and the worst phase arrangements.*

arrangement is at about 2,241 kV/m. The best phase arrangements are at 0.03738 kV/m, as shown in Table 3.

4.2 Magnetic field

All configurations of overhead power transmission lines were installed by MEA as shown in Fig. 2 where all possibilities of phase arrangement produced by MEA overhead power transmission lines for 3-circuit were evaluated using the average current values after phase arrangement technique. Assumptions below were made to simplifying the problems.

- Balanced loads were assumed.
- Both ground and neutral current were ignored.
- The fields measured at 1 m above ground where the x-coordinate range varied from 0 to 50 m were calculated.

The optimal phase arrangement techniques that provide the maximum and minimum magnetic field values generated by MEA overhead power transmission lines using Eqs. (9)–(12) are shown in Figs. 13 and 14, respectively. Fig. 15 shows the comparisons of magnetic field produced by 3-circuit overhead power transmission lines after applying phase arrangement techniques between the worst and the best phase arrangements. However, the worst and best phase arrangements produce magnetic field at 48.83 mG and 10.72 mG, respectively, at the position (0,0) as shown in Table 3.

5. CONCLUSIONS

To minimize the generated electric and magnetic fields, optimal phase arrangement techniques for

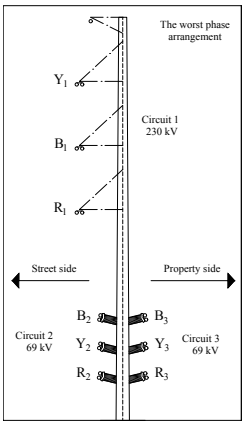

Fig.13: *Maximum magnetic field value provided by the worst phase arrangement.*

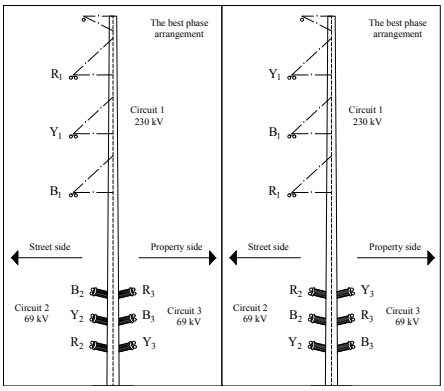

Fig.14: *Proposed best phase arrangements which provide the minimum magnetic field.*

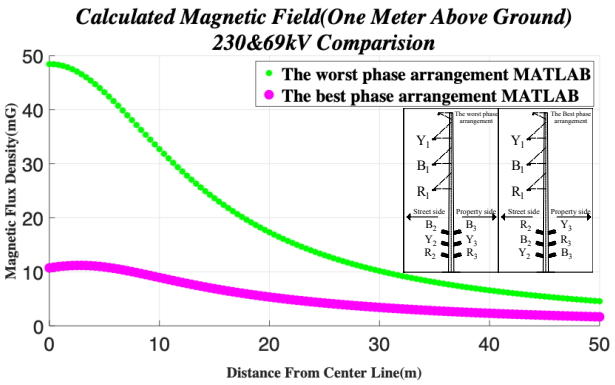

Fig.15: *Comparisons of magnetic field produced by 3-circuit overhead power transmission lines after applying phase arrangement technique between the best and the worst phase arrangements.*

3-circuit MEA overhead power transmission lines (69/230 kV) are proposed. To simplify the problems, the electric and magnetic fields were calculated using an analytical approach derived from equations an implement with 2-D MATLAB. The accuracy of the

derived equations was evaluated by comparing the simulated results with measured results from the South Thonburi power transmission lines at Rama 2 Road (outbound side) evaluated under the same conditions. The comparison results show that the simulated electric field is about 0.4 kV/m higher than that found by measurement at the position (0,0). The value obtained from the simulation of the magnetic field before applying phase arrangement technique is higher than the value from the measurement by MEA by about 6.48 mG, but the simulated result is lower than the measured result by about 0.95 mG at the origin after applying the phase arrangement technique. The result graphs show similar trends. These error values depend on many factors such as real environment, metal fences, trees, towers, electric poles, etc.

The best phase arrangement generates electric and magnetic fields at about 0.03738 kV/m and 10.72 mG, respectively. Those are the lowest electric and magnetic fields values, and lower than that of the limits given by the WHO. Hence, the phase arrangement techniques proposed in this paper can definitely be used as a guideline to reduce both the electric and magnetic fields of MEA overhead power transmission lines.

ACKNOWLEDGMENTS

The authors would like to thank Metropolitan Electricity Authority of Thailand, especially Mr. Jarin Halapee (Electrical Engineer at MEA), for support and assistance. Financial support from the Faculty of Engineering, Srinakharinwirot University, through the research grant No. 228/2561 is acknowledged.

References

[1] World Health Organization report, "Extremely low frequency (ELF) fields," 1984.

[2] International Commission on Non-Ionizing Radiation, "Guidelines for limiting exposure to time-varying electric, magnetic, and electromagnetic fields (up to 300 GHz)," *Health Physics*, vol. 74, no. 4, pp. 494–522, 1998.

[3] Metropolitan Electricity Authority, "Knowledge and understanding of electric and magnetic fields from power lines," Bangkok, Thailand, 2006.

[4] S. M. Korobeynikov, M. S. Akramova, and B. K. Akramov, "Polygraph registration of brain response to magnetic field of power-line frequency," in *2016 2nd International Conference on Industrial Engineering, Applications and Manufacturing (ICIEAM)*, May 2016, pp. 1–4.

[5] A. P. Colbert *et al.*, "Static magnetic field therapy: a critical review of treatment parameters," *Evidence-based complementary and alternative medicine*, vol. 6, no. 2, pp. 133–139, 2009.

[6] S. Mobini, L. Leppik, and J. H. Barker, "Direct current electrical stimulation chamber for treating cells in vitro," *BioTechniques*, vol. 60, no. 2, pp. 95–98, 2016.

[7] S. Korobeynikov, M. Akramova, and B. Akramov, "Polygraph registration of brain response to magnetic field of power-line frequency," in *2016 2nd International Conference on Industrial Engineering, Applications and Manufacturing (ICIEAM)*, 2016, pp. 1–4.

[8] "ELF Electromagnetic Fields and the Risk of Cancer: Report of an Advisory Group on Non-ionising Radiation," *Documents of the NRPB*, vol. 12, no. 1, pp. 1–179, 2001.

[9] International Agency for Research on Cancer and others, "IARC finds limited evidence that residential magnetic fields increase risk of childhood leukaemia," *World Health Organization (WHO)*, no. 136, June 2001.

[10] D. O. Carpenter, "Human disease resulting from exposure to electromagnetic fields," *Reviews on environmental health*, vol. 28, no. 4, pp. 159–172, 2013.

[11] R. McGauchy, "Evaluation of the potential carcinogenicity of electromagnetic fields," *USEPA external review draft EPA/600/6-90 B*, vol. 5, 1990.

[12] "Electromagnetic Fields and the Risk of Cancer: Report of an Advisory Group on Non-ionising Radiation," *Documents of the NRPB*, vol. 3, no. 1, pp. 1–138, 1992.

[13] National Research Council and others, *Possible health effects of exposure to residential electric and magnetic fields*, National Academies Press, 1997.

[14] R. M. Aguiar de Morais Sarmento, "Electric and magnetic fields in overhead power transmission lines," *IEEE Latin America Transactions*, vol. 10, no. 4, pp. 1909–1915, June 2012.

[15] H. Singer, H. Steinbigler, and P. Weiss, "A charge simulation method for the calculation of high voltage fields," *IEEE Transactions on Power Apparatus and Systems*, vol. PAS-93, no. 5, pp. 1660–1668, Sep. 1974.

[16] S. S. Razavipour, M. Jahangiri, and H. Sadeghipoor, "Electrical field around the overhead transmission lines," *World Academy of Science, Engineering and Technology*, vol. 6, pp. 168–171, 2012.

[17] M. Trlep, A. Hamler, M. Jesenik, and B. Stumberger, "Electric field distribution under transmission lines dependent on ground surface," *IEEE Transactions on Magnetics*, vol. 45, no. 3, pp. 1748–1751, March 2009.

[18] A. R. Sinigoj, "On electric and magnetic field under overhead transmission lines," *Elektrotehniški*

Vestnik/Electrotechnical Review, vol. 63, no. 2, pp. 88–93, 1996.

[19] A. Diamantis and A. G. Kladas, "Mixed numerical methodology for evaluation of low-frequency electric and magnetic fields near power facilities," *IEEE Transactions on Magnetics*, vol. 55, no. 6, pp. 1–4, June 2019.

[20] J. Gonos *et al.*, "Environmental impact analysis of electric power lines," in *2018 IEEE International Conference on Environment and Electrical Engineering and 2018 IEEE Industrial and Commercial Power Systems Europe (EEEIC/I&CPS Europe)*, 2018, pp. 1–5.

[21] S. Nunchuen, J. Halapee, and V. Tarateeraseth, "Electric field minimization using optimal phase arrangement techniques for mea overhead power transmission lines," in *2019 16th International Conference on Electrical Engineering/Electronics, Computer, Telecommunications and Information Technology (ECTI-CON)*, 2019, pp. 325–328.

[22] Department of MEA Research and Development, "Electric field inspection and magnetic field before and after the phase arrangements of south thonburi transmission lines, 69 kV 2 circuits, Rama 2 road (outbound side)," Metropolitan Electricity Authority, Bangkok, Thailand, May 2002.

[23] V. Tarateeraseth, *Electromagnetic Fields*, Bangkok, Thailand: Aksorn Sampan (in Thai), 2014.

[24] F. S. Young, *Electric and Magnetic Field Management Reference Book*, Palo Alto, CA, USA: EPRI, 1999.

[25] *IEEE Standard Procedures for Measurement of Power Frequency Electric and Magnetic Fields from AC Power Lines*, IEEE Standard 644-1994, Nov. 1994.

Suthasinee Nunchuen received her B.Eng. and M. Eng. degrees in electrical engineering from Srinakharinwirot University (SWU), Bangkok, Thailand, in 2017 and 2020, respectively. Currently, her research interests are mainly focused on electromagnetic compatibility in power systems and biological effects of electromagnetic fields.

Vuttipon Tarateeraseth received his B. Eng. (second-class honors) and M. Eng. degrees in electrical engineering from King's Mongkut Institute of Technology Ladkrabang (KMITL), Thailand, and his Ph.D. in Information and Communication Technologies from Polytechnic University of Turin, Italy. He was a visiting researcher at the Nanyang Technological University, Singapore, from July 2008 to July 2009. Currently, he is an Associate Professor in the Department of Electrical Engineering at Srinakharinwirot University, Thailand. His research interests are mainly in the fields of Power Electronics and Electromagnetic Compatibility.